Complex analog correlating pulsed UWB-receiver in realistic 0-1GHz channels

Marian Verhelst* and Wim Dehaene
Katholieke Universiteit Leuven - ESAT-MICAS
Kasteelpark Arenberg 10, B-3001 Heverlee, Belgium
Email: mverhels@esat.kuleuven.ac.be
*M. Verhelst is Research Assistant of the Fund for Scientific Research - Flanders (Belgium)(FWO-Vlaanderen)

Abstract

The complex analog correlating (CAC) receiver is an excellent candidate for low power, low data rate pulsed UWB communication, but only in ideal AWGN channels. This paper adapts the traditional architecture and acquisition scheme of this receiver for operation in realistic multipath channels. Two schemes are presented: a high performance scheme, and a simpler, but easy to implement and low power scheme. Monte-Carlo simulations illustrate the performance improvement in realistic 802.15.4a (LOS and NLOS) channels. The receiver's power consumption can be traded for performance by tuning the number of resolved path components. The system outperforms the traditional CAC receiver and the transmitted reference receiver in all environments.

1. Introduction

Pulsed ultra wideband (UWB) communication [1] has attracted a lot of attention from the research community after its approval by the FCC [2]. Not only does this wide bandwidth (of at least 500MHz, up to 7GHz) allow communication with very high data rates. It also results in the capability of very accurate localization, robustness against fading and multipath channels and simple, low power transmitter and receiver designs. As a result, ultra-wideband becomes increasingly popular for power efficient ranging, imaging and distance measurement with communication at low data rates. In this application domain, the main implementation issues are the power consumption and robustness rather than achieving high data rates.
Numerous ultra-wideband architectures have been proposed in the literature. Although the fully digital receiver [3] and the traditional analog correlation receiver [4] are the most common, none of them is suited for operation when power consumption and robustness are the primary concerns. The fully digital receiver requires high ADC speeds and hence power consumption, while the traditional analog correlation receiver has problems with multipath channels. Transmitted reference systems [5] perform very well in multipath environments, without needing a fast ADC. Their performance however degrades rapidly in noisy environments. Moreover, they need long, accurate analog delay lines, which are difficult to fabricate.
[6] and [7] introduced an analog correlation receiver, that correlates the incoming pulses with a windowed sine. The proposed architecture does not need a high speed ADC or DAC and as a result has a very low power consumption. While it captures the signal energy very good in ideal (AWGN) channels, this receiver however suffers from serious performance degradation in realistic multipath environments. This, like most analog correlating receivers, due to its inability to capture multiple path components. This paper will start from this complex analog correlation receiver, but extends the existing architecture to be able to do multipath recombination. The result is a low power receiver, with a good performance in realistic channels. The receiver performance will be evaluated with Monte-Carlo simulations in realistic LOS and NLOS channels for the 0-1GHz range. Finally its performance will be compared to the performance of the transmitted reference system.

2. System description

2.1. Data representation

The transmitted waveform in pulsed ultra wideband communications, with BPSK data modulation, is given by

$$s_{tx}(t) = \sum_{n=-\infty}^{\infty} b_n \sum_{k=0}^{N_s-1} a_k \sqrt{E_p} w_{tx}(t - kT_p - nT_s) \quad (1)$$

with pulse repetition period T_p, symbol period $T_s = N_s T_p$, total energy per pulse E_p. $b_n \in \{-1, 1\}$ and $a_k \in \{-1, 1\}$ are respectively the n^{th} transmitted information bit and the k^{th} bit of the used spreading code of length N_s. $w_{tx}(t)$ is the transmitted pulse form, with unit energy

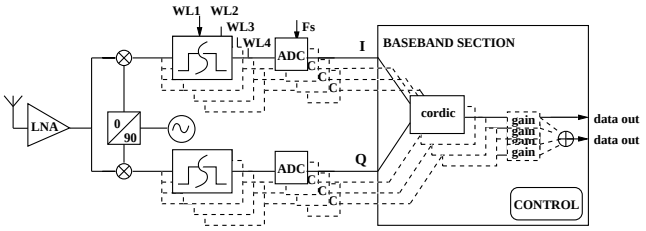

Fig. 1. The complex analog correlation (CAC) receiver, full lines: as introduced in [7], dashed lines: proposed multipath CAC with $L_{an} = 4$

($\frac{1}{T_p}\int_0^{T_p} w_{tx}^2(t)\,dt = 1$). Without loss of generality a second derivative gaussian pulse is assumed in our simulations. The received signal will be denoted as

$$s_{rx}(t) = \sum_{n=-\infty}^{\infty} b_n \sum_{k=0}^{N_s-1} a_k \sqrt{E_p} w_{rx}(t - kT_p - nT_s) + n(t) \quad (2)$$

with $n(t)$ additive gaussian noise (AWGN) with zero mean and power spectral density $\frac{N_0}{2}$ over the bandwidth W of the receiver. $w_{rx}(t)$ is the pulse waveform, corrupted by the channel and antenna transfer function. The received pulse waveform $w_{rx}(t) = w_{tx}(t) \otimes h(t) = \sum_{l=0}^{L-1} \alpha_l w_{rx,l}(t - \tau_l)$ is composed of L path components arriving at the receive antenna with associated attenuation α_l and delay τ_l. The received multipath components are denoted by $w_{rx,l}(t)$, which differ from the transmitted pulse $w_{tx}(t)$ due to waveform distortion introduced by the frequency selectivity of the medium and the antennas. We assume that T_p is large enough to avoid inter pulse interference.

2.2. Complex analog correlation receiver

An optimal ultra wideband receiver would implement a matched filter to detect the received data bit. The incoming signal is here correlated with a locally stored template, equal to $w_{rx}(t)$. The determination and generation of this template is however very power consuming. Therefore, the ideal template signal is replaced by a template signal that is much easier to generate in [7].

The receiver architecture proposed in [7] is plotted in figure 1. The incoming pulses are multiplied with a sine, followed by a windowed integration. The integration result is sampled at the end of every pulse period. In the time domain, this is equivalent to the correlation with a windowed sine wave. To speed up acquisition and relax the timing constraints on the receiver and transmitter clock, the incoming pulses are at the same time correlated with a windowed cosine. A cordic is used in the digital domain to recombine the energy of the in-phase and quadrature path. Because of the two orthogonal paths in the frontend, we will denote this receiver by *complex analog correlation (CAC) receiver*.

The matching template in this receiver $w_T(t)$, with which the incoming pulses are correlated, can hence be written as:

$$w_T(t) = \begin{cases} cos(\omega_c t) + i\, sin(\omega_c t) & 0 < t < L_w \\ 0 & else \end{cases} \quad (3)$$

with L_w the length of the analog integration window, $\omega_c = 2\pi f_c$ and f_c the oscillator frequency. The receiver, as proposed in [7], works with a fixed integration window length and sine frequency. During acquisition the integration window is slid over the complete pulse period in steps T_{step}. For every position a correlation with the incoming signal is done. The position of the window will be fixed to the multiple of T_{step} that gives the largest correlation energy.

During data reception, the correlation result of N_s pulse periods will be combined to detect the received bit. The decision variable for the n^{th} bit can be expressed as:

$$r_{CAC}(n) = \int_0^{T_s} s_{rx}(t + nT_s) \sum_{k=0}^{N_s-1} a_k w_T(t - kT_p)\,dt \quad (4)$$

The decision variable r_{CAC} is gaussian, with conditional mean $E[r_{CAC}(n)|b_n] = b_n N_s \sqrt{E_p E_T \eta_{CAC}}$, with E_T the energy of the template signal and η_{CAC} the energy capture efficiency of the receiver ([8]). The latter shows how well the matching template matches the incoming signal:

$$\eta_{CAC} = \frac{[\int_{-\infty}^{\infty} w_{rx}(t) w_T(t)\,dt]^2}{\int_{-\infty}^{\infty} w_{rx}^2(t)\,dt \int_{-\infty}^{\infty} w_T^2(t)\,dt} \quad (5)$$

Since the matching template is not equal to the received signal $w_{rx}(t)$, η_{CAC} will be smaller than 1. This loss can however be limited by carefully selecting the window length and the sine frequency.

The variance of the noise term can be computed as:

$$\begin{aligned} \sigma_{N_{CAC}}^2 &= \sum_{k=0}^{N_s-1} E[\int_0^{T_p} n(t) w_T(t)\,dt \int_0^{T_p} n(u) w_T(u)\,du] \\ &= N_s E_T \frac{N_0}{2} \end{aligned} \quad (6)$$

As a result the bit error probability (Pe) of the receiver can be written as:

$$Pe_{CAC} = Q(\sqrt{\frac{2N_s E_p \eta_{CAC}}{N_0}}) \quad (7)$$

with $Q(x) = (1/\sqrt{2\pi}) \int_x^{\infty} exp(-t^2/2) dt$ for $x > 0$

Except for the factor η_{CAC} this error probability is the same as for the optimal, matched filter receiver (for which $\eta_{CAC} = 1$).

Figure 2 shows the performance of these two receivers, based on Monte-Carlo simulations and based on the analytical expression (7). In these simulations $N_s = 1$, $L_w = 4ns$, $f_c = 350MHz$. The simulations show a performance degradation of approximately 1dB due to imperfect matched filtering. Hence, in this receiver the power consumption is reduced drastically by reducing the ADC sampling speed up to pulse rate, while only marginally degrading its performance.

Up to now, the CAC receiver has only been studied in AWGN channels. In realistic environments however, multipath effects have to be taken into account. The receiver

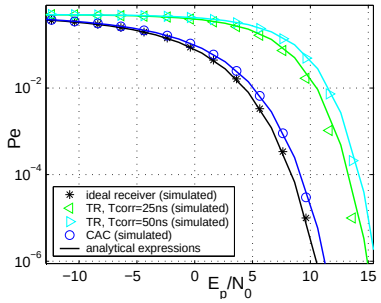

Fig. 2. Bit error probability in AWGN environment vs. E_p/N_0, $N_s = 1$, $T_p = 50ns$ for an ideal, a CAC and a transmitted reference (TR) receiver

proposed in [7] will in these environments only capture the energy of the strongest path. As shown by many authors ([9]), this seriously affects the performance of the receiver and can result in an additional degradation compared to perfect matched filter reception of up to more than 10dB. Next paragraph will describe modifications to the existing receiver to improve the receiver performance in multipath environments.

3. Multipath complex analog correlating receiver

3.1. Ideal multipath CAC receiver

In multipath environments, L path components $\alpha_l w_{rx,l}(t-\tau_l)$ will arrive at the receive antenna, all with a different delay and attenuation. The correlation of a single path component corrupted by noise, $(\alpha_l w_{tx,l}(t-\tau_l)+n(t))$, with the windowed sine and cosine results in the values I_l and Q_l.

$$I_l = \int_{\tau_l}^{\tau_l+L_w} (\alpha_l w_{rx,l}(t-\tau_l)+n(t))cos(\omega_c t)\,dt \qquad (8)$$

$$Q_l = \int_{\tau_l}^{\tau_l+L_w} (\alpha_l w_{rx,l}(t-\tau_l)+n(t))sin(\omega_c t\,dt) \qquad (9)$$

As a result, every multipath component can be represented as a vector in the constellation diagram, with amplitude $A_l = \sqrt{(I_l)^2+(Q_l)^2}$ and phase $\phi_l = arg(I_l, Q_l)$.
Unlike a transmitted reference system, the CAC receiver cannot capture all the energy of the different paths by simply opening the analog integration window longer. Because the phase ϕ_l and the amplitude A_l of the different path components is different after correlation, energy would be lost when collecting them on the same integrator. Therefore, for optimal detection, the energy of all these different paths has to be detected separately and recombined in the digital domain by a weighted addition of the amplitudes of these path vectors. This results in the decision variable for the ideal multipath CAC (IMCAC) receiver:

$$r_{IMCAC}(n) = b_n \sum_{0}^{L-1} \beta_l (I_l + jQ_l) \qquad (10)$$

The variables β_l are equivalent to the filter tap coefficients in a Rake receiver. The output signal to noise ratio of the receiver is hence maximized by choosing them as $\beta_l = (\overline{I_l} + j\overline{Q_l})^* = (\overline{I_l} - j\overline{Q_l}), \forall l \in [0, L-1]$ (x^* denoting the complex conjugate and $\overline{x}$ denoting the expected value of x). In this way the receiver optimally captures the energy of all the path components. As a result, the loss in relation to perfect matched filtering will be equal to the loss of the traditional CAC receiver in AWGN channels. This is because the only loss factor is the imperfect matching between the received pulses and the windowed sine.
While the IMCAC receiver performs excellent in multipath environments, it requires $2L$ analog branches in the receiver frontend: one I- and one Q-channel for every captured path. Since the number of multipath components can be very large ([9]), it is in reality impossible to implement this receiver.

3.2. Proposed multipath CAC receiver

The receiver proposed here, is based on the IMCAC receiver. The number of analog branches in the receive frontend will however be limited to $2L_{an}$. Increasing L_{an} will increase the performance as well as the power consumption of the receiver. The designer can, depending on the environment, the desired performance and the maximal power consumption, select the optimal value of L_{an}. The receiver architecture is plotted in figure 1 (dashed lines) for $L_{an} = 4$.
To reduce the number of analog branches in the receiver front end to $2L_{an}$, different path components will be captured by the same analog branch. Therefore, the integration window of the integrator in every branch will be opened more than once in every pulse period. The ADCs still sample the integration results at the end of every pulse period. The resulting I_k and Q_k value for branch k at the input of the digital domain, will hence be:

$$I_k = \int_0^{T_p} (w_{rx}(t)+n(t))u_k(t)cos(\omega_c t)\,dt \qquad (11)$$

$$Q_k = \int_0^{T_p} (w_{rx}(t)+n(t))u_k(t)sin(\omega_c t)\,dt \qquad (12)$$

with window signal $u_k(t) = \sum_{m=0}^{\lceil \frac{T_p}{T_r} \rceil - 1} u(t-mT_r)$, T_r the time resolution with which the integrator can be activated and $u(t)$ the unit window of length T_r.
The correlation result of multiple path components will hence be added on the same integrator. This results in a performance degradation in comparison to the IMCAC receiver, where the recombination is done in the digital domain. There are two reasons for this loss:

1) The constellation vectors of all path components captured by the same branch are added in the analog domain. This is suboptimal when the captured components have a different phase ϕ_l.

2) All path components captured by the same branch get the same weight in the final decision variable. This is suboptimal when the captured components have a different amplitude A_l.

To minimize the loss due to these two effects and maximize the output performance of this receiver, the path components will in a first step be divided over the different analog branches based on their phase ϕ_l. Vectors with similar phases should be integrated on the same branch. Secondly, components that do not contribute enough to the signal energy captured by a branch should be rejected, since integrating them also results in collecting additional noise.
From now on, we will denote a set of path components captured by the same analog branch as a *correlation group* and the corresponding (complex) correlation result as a *correlation vector*.

1) PD-MCAC acquisition algorithm: The construction of the correlation groups is done during an acquisition phase of the receiver, before data communication. The acquisition of the MCAC receiver with $2L_{an}$ branches contains four steps: In the first step, the receiver learns the channel. Since the time resolution with which the integrators can be activated and deactivated is equal to T_r, it makes no sense to scan the channel with a finer resolution. As a result, the total pulse period is split into $\lceil \frac{T_p}{T_r} \rceil$ time frames of T_r seconds. For every time frame k, I_k^{av} and Q_k^{av} are searched by averaging the correlation result over N pulses:

$$I_k^{av} = \frac{1}{N} \sum_{i=1}^{N} \int_{iT_p+(k-1)T_r}^{iT_p+kT_r} (w_{rx}(t) + n(t)) cos(\omega_c t)\, dt \quad (13)$$

$$Q_k^{av} = \frac{1}{N} \sum_{i=1}^{N} \int_{iT_p+(k-1)T_r}^{iT_p+kT_r} (w_{rx}(t) + n(t)) sin(\omega_c t)\, dt \quad (14)$$

(15)

Increasing N will improve the channel estimation. The result is a set of $\lceil \frac{T_p}{T_r} \rceil$ constellation vectors, that will de denoted as the *bin vectors*. This information will be used in the second step of the acquisition.
When the bin vectors are known, they have to be grouped in L_{an} correlation groups. This is done based on a clustering algorithm. The algorithm will try to cluster the bin vectors $(I_k^{av}, Q_k^{av}), \forall k \in [1, .., \lceil \frac{T_p}{T_r} \rceil]$ into L_{an} clusters C_j with correlation vectors $c_j = (I_{c_j}, Q_{c_j}), \forall j \in [1, .., L_{an}]$, so that the sum of squared distances of every bin vector to its correlation vector is minimized:

$$min \sum_{j=1}^{L_{an}} \sum_{i=1}^{\#C_j} ||s_i^{(j)} - c_j||_\phi^2 \quad (16)$$

with $\#C_j$ the number of vectors in C_j and $s_i^{(j)}$ the i^{th} vector in C_j. The distance metric $||.||_\phi$ between two vectors used here is the phase difference between the vectors. The amplitude information of a vector is not used in this step.

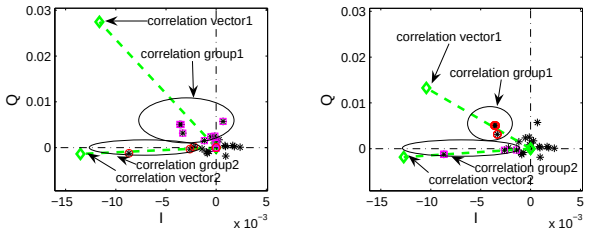

(a) PD-MCAC receiver (b) LP-MCAC receiver

Fig. 3. Comparison of acquisition with the PD-CACR and the LP-CACR for an NLOS channel and $L_{an} = 2$. $*$ = bin vectors, $\diamond$ = correlation vectors.

The clustering algorithm chosen is the K-means clustering [10]. This algorithm is preferred above other clustering techniques, because it is simple and offers good results when the number of clusters is known on beforehand. The latter is the case in the MCAC receiver, where the number of clusters is equal to L_{an}. The third step in the acquisition process will iteratively prune every correlation group. A component k should be rejected from the correlation group C_j, if it decreases the signal to noise ratio of the correlation result, or if:

$$\frac{(A_{C_j} - A_k cos(\phi_{C_j} - \phi_k))^2}{\frac{N_0}{2}(|C_j| - 1)} > \frac{(A_{C_j})^2}{\frac{N_0}{2}(|C_j|)} \quad (17)$$

$$A_k cos(\phi_{C_j} - \phi_k) < (1 - \sqrt{\frac{|C_j| - 1}{|C_j|}}) A_{C_j} \quad (18)$$

with A_{C_j} and ϕ_{C_j} the amplitude and the phase of the correlation vector c_j, which is the sum of all bin vectors assigned to this correlation group.
After the third step in the acquisition algorithm, there exist L_{an} distinct correlation groups, all containing one or more bin vectors. This situation is plotted in figure 3(a) for a NLOS channel and $L_{an} = 2$, in which the bin vectors $(*)$ belonging to one of the two correlation groups are indicated. Since every bin vector corresponds to one time frame of length T_r, it is straightforward to determine the window signals for every correlation group. These window signals will control the analog correlators of the $2L_{an}$ branches in the frontend during data reception. In the digital domain the amplitude A_{C_j} of all L_{an} correlation vectors c_j will be combined. The weight β_{C_j} given to every vector c_j is proportional to the square root of its signal to noise ratio, or:

$$\beta_{C_j} = \frac{A_{C_j}}{\sqrt{\#C_j}} \quad (19)$$

Section 4 will show that the performance of this multipath complex analog correlating receiver is very good and converges to the ideal matched filter performance for $L_{an} \to \infty$ and $T_r \to 0$. Since this receiver tries to get the

optimal performance for a given number of analog branches L_{an}, we will denote it with *performance driven multipath CAC receiver* (PD-MCAC). The acquisition algorithm proposed in this section is however very computational intensive. In the targeted application domain, the power consumption of the receiver is of primary concern. The huge amount of on-chip comparisons and additions needed in the iterative K-means clustering algorithm and the pruning step are undesirable. Next section will introduce a simplified, *low power* acquisition algorithm (LP-MCAC). In section 4 the performance of the two approaches will be compared.

2) LP-MCAC acquisition algorithm: To reduce the necessary computational power during the acquisition phase, the clustering and pruning of the acquisition process will be be simplified. In the LP-MCAC acquisition algorithm, the number of additions and comparisons is reduced drastically at almost no performance degradation. This algorithm is however only applicable for $L_{an} \leq 4$. This is not necessarily a problem, since it is not very likely that more than 8 analog branches will be tolerated in low power applications. Moreover, section 4 will show that making L_{an} larger than 4 only improves the performance marginally.

The iterative K-means clustering algorithm will be replaced by a one-step division of the bin vectors into 4 separate correlation groups. There is one correlation group for every quadrant of the constellation diagram. Every bin vector will be assigned to the correlation group of the quadrant it is situated in. This clustering needs hardly any computations, since it only looks at the sign of every I and Q value. If $L_{an} < 4$, only the L_{an} correlation groups with the most energy will be used. Although the clustering is very rough, section 4 will reveal good results. The reason lies in the fact that also in the PD-MCAC algorithm vectors more than $\frac{\pi}{2}$ radians apart will hardly ever be assigned to the same constellation group.

To also reduce the computational effort of the pruning step, the bin vectors will be removed from the correlation group if their amplitude is smaller than 0.5 times the amplitude of the largest vector in that correlation group. In this way the computation of the phase difference $(\phi_{C_j} - \phi_k)$ and the cosine of it are avoided. Finally, the weight of every correlation result is again derived by formula (19).

Figure 3(b) shows the result of the LP-MCAC acquisition for the same NLOS channel. Although this acquisition method only groups bin vectors in the same quadrant of the constellation diagram and prunes differently, it still results in similar and quite good correlation vectors in comparison the the PD-MCAC scheme.

4. Simulation results and comparison to TR

In this section the performance MCAC receiver will be evaluated based on Monte-Carlo simulations and compared

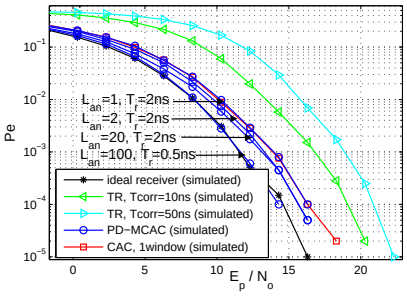

Fig. 4. PD-MCAC bit error probability in LOS environment vs. E_p/N_0, $N_s = 1$, $T_p = 50ns$, ideal channel knowledge

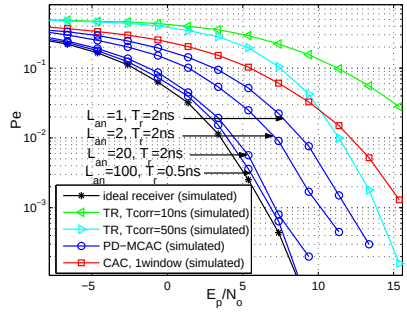

Fig. 5. PD-MCAC bit error probability in NLOS environment vs. E_p/N_0, $N_s = 1$, $T_p = 50ns$, ideal channel knowledge

against the transmitted reference system (TR) [5], another low power pulsed UWB receiver. The performance will be evaluated in line of sight channels (LOS) and non line of sight channel (NLOS). The channel models used are the models proposed by the IEEE 802.15.4a task group for 0-1GHz channels [11]. For every environment (LOS and NLOS), the average performance over 100 channels and 20.000 pulses is taken. Ideal channel knowledge is assumed in the simulations. The pulse template used here is the second derivative gaussian pulse, with a -10dB bandwidth of 600MHz in the 0-1GHz band. The pulse rate is 20MHz ($T_p = 50ns$), $N_s = 1$. All figures in this section plot the bit error probability (Pe) vs. E_p/N_0. The energy per pulse is used here instead of the energy per bit, to avoid favoring the MCAC receiver over the transmitted reference (TR) receiver. While the TR receiver needs two pulses for every bit, the MCAC receiver also has some overhead for training and synchronization.

Figure 4 shows the average bit error probability (Pe) at the PD-MCAC receiver output in a LOS environment for different values of L_{an}. The plot also contains the performance curve of the traditional CAC receiver, that captures only the strongest path component. In this environment, most of the signal energy is concentrated in the first, direct path. As a result, the performance of the CAC receiver is already quite good. Although in the limit ($L_{an} \rightarrow \infty$ and $T_r \rightarrow 0$), the performance of the PD-MCAC receiver becomes equal to

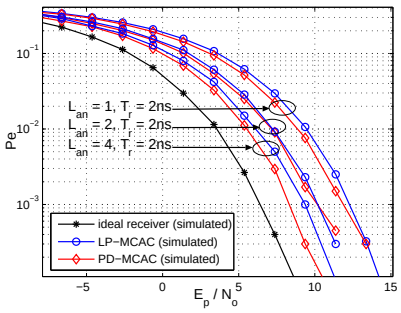

Fig. 6. Comparison of PD-MCAC and LP-MCAC performance in NLOS environment, $N_s = 1, T_p = 50ns$, ideal channel knowledge

the ideal matched filter performance, it is clear that it is not worth it to use an MCAC receiver in this LOS environment. The performance of the same receiver in a NLOS environment is plotted in figure 5. The degradation of the bit error probability for the CAC receiver is much worse now, since there is no single strongest path anymore. The PD-MCAC receiver with $L_{an} = 1$ already improves the performance significantly. The multipath recombination technique presented in this paper can hence, even without adding additional circuitry, already gain 4dB in relation to the CAC receiver. L_{an} can be increased to shift closer and closer to the ideal matched filter curve. This flexibility can be used by the designer to trade power for performance.

Figure 6 compares the LP-MCAC and the PD-MCAC receiver in a NLOS environment. The loss of this simplified, low power LP-MCAC receiver in relation to the complex PD-MCAC receiver is limited to less than 1dB for the same number of analog branches L_{an}. L_{an} is limited to 4 in the LP-MCAC receiver. However, as can be seen, the gain of increasing L_{an} becomes smaller for large L_{an}. This makes large L_{an} unattractive, since the increase in power consumption is not worth the marginal gain resulting from it.

Figures 2, 4 and 5 all also contain the bit error probability curves for the transmitted reference (TR) receiver, proposed in [5]. This receiver correlates the incoming signal with a delayed version of itself, instead of using a stored reference. In this way channel estimation is not required, what results in good performance in multipath environments. Its major drawback however is the noise-cross-noise term that appears in the correlator output, which severely degrades the performance at low E_p/N_0. This receiver is also a good candidate for low power, low data rate applications, since it does not need any mixers, oscillators or fast ADCs. While its power consumption is probably lower than the one of the MCAC receiver, its performance is much worse, as can be seen from the different plots. Moreover, the TR receiver is also less scalable, since there is no way to improve the performance by consuming some additional power. The only parameter that can be tuned is the length of the integration window T_{corr}. Reducing T_{corr} helps to reduce the noise-cross-noise term, but at the same time reduces the captured signal energy. The possible gain of tuning this parameter is hence rather limited. Finally note that the plots are made for $N_s = 1$ and that the difference between the two receivers will only increase for larger N_s in favor of the MCAC receiver, due to the shift to lower E_p/N_0 regions. This makes the LP-MCAC receiver much more attractive than the TR system for robust, low power communication.

5. Conclusion

This paper presents a novel way to do multipath data reception in a complex analog correlating receiver. An architecture together with two novel acquisition schemes are proposed. The first PD-MCAC algorithm offers the best performance and converges to the matched filter bound when the number of analog integrators increases. In the alternative, LP-MCAC acquisition method, the computational cost is reduced significantly at the cost of only a slight decrease in performance. Monte-Carlo simulations of the proposed receiver with both acquisition schemes are presented and compared against the traditional CAC receiver and the transmitted reference system. The simple, low power LP-MCAC receiver offers good performance in multipath channels. The freedom in choosing the number of analog branches in the frontend can be used by the designer to trade performance for power.

References

[1] M. Win and R. Scholtz, "Impulse radio: How it works," *IEEE Communications Letters*, vol. 2, no. 2, pp. 36–38, Feb. 1998.

[2] FCC, "First report and order," FCC 02-48, February 14, 2002.

[3] I. O'Donnell, M. Chen, S. Wang and R. Brodersen, "An integrated, low-power, ultra-wideband transceiver architecture for low-rate, indoor wireless systems," *IEEE CAS Workshop on Wireless Communications and Networking*, Sept. 2002.

[4] M. Win and R. Scholtz, "Ultra-wide bandwidth time hopping spread-spectrum impulse radio for wireless multiple-access communications," *IEEE Transactions on Communications*, vol. 48, no. 4, pp. 679–691, Apr. 2000.

[5] R. Hoctor and H. Tomlinson, "Delay-hopped transmitted reference RF communications," *Proceedings of the IEEE Conference on Ultra Wideband Systems and Technologies*, pp. 265–270, May 2002.

[6] S. Lee, "Design and analysis of ultra-wide bandwidth impulse radio receiver," 2002, ph.D. Dissertation EE, USC.

[7] M. Verhelst and W. Dehaene, "System design of an ultra-low power, low data rate, pulsed uwb receiver in the 0-960mhz band," in *IEEE International Conference on Communications, 16-20 May*, vol. 4, 2005, pp. 2812 – 2817.

[8] R. Scholtz, D. Pozar and W. Namgoong, "Ultra-wideband radio," *EURASIP Journal of Applied Signal Processing*, vol. 3, pp. 252–272, 2005.

[9] A. Rajeswaran, V. Somayazulu and J. Foerster, "RAKE performance for a pulse based UWB system in a realistic UWB indoor channel," in *ICC, 2003*, vol. 4, May 2003, pp. 2879– 2883.

[10] J. McQueen, "Some methods for classification and analysis of multivariate observations," *Computer and Chemistry*, vol. 4, pp. 257–272, 1967.

[11] IEEE802.15.4a, "15-04-0505-04-004a-UWB-Channel-Model-for-under-1-GHz," 2004, www.ieee802.org/15/pub/TG4a.html.